Theoretical Study of the Electronic Properties of Nb_6I_9S and $Nb_6(H)I_9S$

H.-Jürgen Meyer*,[†] **and John D. Corbett***,[‡]

Institut für Anorganische Chemie, Universität Hannover, 3000 Hannover 1, Germany, and
Department of Chemistry, Iowa State University, Ames, Iowa 50011

Received August 6, 1991

The structures of the recently synthesized new chain compounds Nb_6I_9S and $Nb_6(H)I_9S$ show interesting distortions from what might be viewed as their ideal arrangements. These have been studied in more detail by extended Hückel calculations on the quasi-one-dimensional chain structures. The electronic structures for the observed crystal structures are compared with that of a hypothetical undistorted structure that also contains two Nb_6I_9S clusters per repeating unit in the infinite chain. Considering 20 electrons/ideal cluster, a local half-filled block is formed by four bands that become 4-fold degenerate at the zone edge. In the distorted structures degeneracies break off to yield a two (empty) over two (filled) band splitting in $Nb_6(H)I_9S$ (20 electrons per cluster) and a three (empty) over one (filled) band splitting in Nb_6I_9S (19 electrons per cluster). Thus electronic effects are responsible for the observed distortions.

Introduction

Many low dimensional compounds show distorted structures that are often classified as the result of a Peierls distortion, or a charge-density-wave phenomenon. A classic example is the pairing distortion of niobium atoms along the infinite chains in NbX_4 (X = Cl, Br, I).[1] Similar distortions have been studied for NbI_3, ZrI_3[2] and NbZ_3 (Z = S, Se).[3]

Recently, detailed studies of the one-dimensional infinite chain structure of the octahedral $(Nb_6I_6S_{2/2})I_{6/2}$ cluster revealed distortions of the cluster framework and at the sulfur bridge.[4] The incorporation of a hydrogen atom into octahedral interstices occurs with subtle geometrical changes. A significant and distinct distortion pattern was reported for the isolated clusters in Nb_6I_{11}[5–7] and, of course, in numerous other cluster compounds that deviate from their "ideal" electron count. With 24 electrons in metal–metal bonding states, an M_6X_8 type cluster is expected to be undistorted (and with 14 or 16 electrons for a M_6X_{12} cluster); thus distortions, if present, may not be driven electronically.

In Nb_6I_9S, 19 electrons per cluster are present in metal–metal bonding states, and 20 electrons are present in the corresponding hydride. The incorporation of a nitrogen atom as an interstitial atom instead would lead to a 24-electron count, which is also present in $Mo_6I_8Se_2$.[8] Structural work on $Mo_6I_8Se_2$ indeed suggests that an undistorted trigonal antiprismatic cluster occurs in the same basic structural framework as obtained for Nb_6I_9S.

In the present study, we trace the electronic conditions that cause slight but distinct distortions in Nb_6I_9S and its hydride, using tight-binding extended Hückel calculations.[9] We also discuss the distortions involving intercluster Nb–Nb interactions and the conductivity properties influenced therefrom. The bonding characteristics of the interstitial hydrogen atoms are presented as well as the magnetism of Nb_6I_9S and $Nb_6(H)I_9S$.

Structures of Nb_6I_9S and $Nb_6(H)I_9S$

Nb_6I_9S and $Nb_6(H)I_9S$ form distorted chain structures of unexpected low symmetry ($P\bar{1}$). Each infinite chain contains two differently aligned, but nearly equivalent, $Nb_6I_6S_2$ octahedra that are bridged by inner sulfur and outer iodine atoms to produce $(Nb_6I_6S_{2/2})I_{6/2}$ (Figure 1). Hydrogen in $Nb_6(H)I_9S$ is presumed to be located at a center of symmetry in the middle of each cluster. Adjacent chains interact only via van der Waals forces (Figure 2), meaning that a study of a single chain is sufficient to gain information about bonding and stability. Two clusters along the infinite chain ([111] direction) have to be taken for consideration in the one-dimensional Brillouin zone.

The unusual feature of the structures are distortions of the metal octahedra. Normally for this structural arrangement we would expect regular trigonal antiprisms of niobium atoms interconnected by a trigonal prism formed by niobium triangles of adjacent clusters with a sulfur atom in its center. The main deformation pattern obtained in Nb_6I_9S is a compression of clusters along opposite vertices (Nb1–Nb1′ and Nb5–Nb5′) and elongation of their waist planes (Figure 3), yielding four short and two long metal–sulfur bonds and two short and one long metal–metal contacts between adjacent clusters (Figure 1). In $Nb_6(H)I_9S$, the clusters become more symmetrical via a sizable anisotropic expansion, particulary a drastic increase of about 0.5 Å along the compression axes noted above. Angles within the waist planes (Nb2, Nb2′, Nb3, Nb3′ and Nb4, Nb4′, Nb6, Nb6′) now deviate by 2° from 90°, increasing the intracluster distances Nb2–Nb2′ and Nb4–Nb4′ (Figure 3).

Using distances to judge the bond situation in Nb_6I_9S, each cluster forms four strong and two weaker metal–sulfur bonds (Table I). Adjacent clusters exhibit two weak metal–metal interactions, whereas the remaining pair of niobium atoms of each cluster form shorter intracluster bonds instead. The latter is supported by a shift of vertices (Nb1, Nb1′, Nb5, Nb5′) away from adjacent sulfur atoms and by sulfur atoms being slightly off the axis of the Nb_6 stacks (0.19 Å in Nb_6I_9S).

Results

For understanding the principal bonding situations in terms of orbitals, we refer to an idealized structure. The idealized structure can be considered to contain stacks of two (staggered) Nb triangles (point group D_{3d}) that form one cluster and are capped by one sulfur atom. The second cluster forming the repeat unit of the infinite chain results from applying a $6_3/m$ operation on the parent.

The metal–metal bonding is based on interactions of niobium 4d (5s, 5p) orbitals, as affected by orbital mixing with sulfur and

---

[†] Universität Hannover.
[‡] Iowa State University.
(1) Whangbo, M. H.; Foshee, M. J. *Inorg. Chem.* **1981**, *20*, 113.
(2) Dorhout, P. K.; Corbett, J. D. *Inorg. Chem.* **1991**, *30*, 1467.
(3) Boswell, F. W.; Prodan, A. *Physica B+C* **1980**, *99*, 361.
(4) Meyer, H.-J.; Corbett, J. D. *Inorg. Chem.* **1991**, *30*, 963.
(5) Bateman, L. R.; Blount, J. F.; Dahl, L. F. *J. Am. Chem. Soc.* **1966**, *88*, 1082.
(6) Simon, A.; von Schnering, H.-G.; Schäfer, H. *Z. Anorg. Allg. Chem.* **1967**, *355*, 295.
(7) Imoto, H.; Simon, A. *Inorg. Chem.* **1980**, *19*, 1241.
(8) Perrin, C.; Sergent, M. *J. Chem. Res. Miniprint* **1983**, 38.
(9) Hoffmann, R. *Solids and Surfaces: A Chemist's View of Bonding in Extended Structures*; VCH: New York, 1988.

0020-1669/92/1331-4276$03.00/0

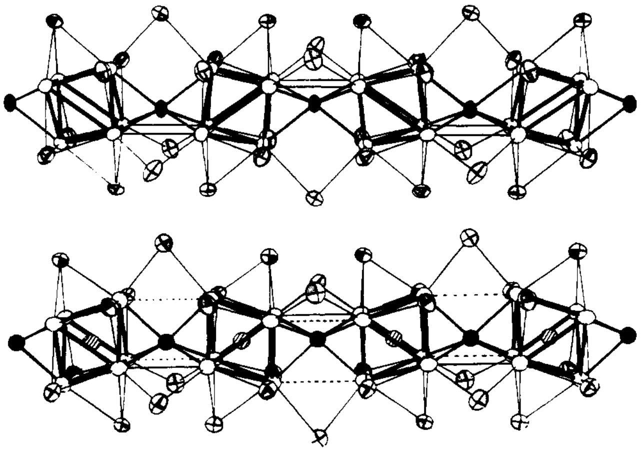

Figure 1. Section of the infinite chains in Nb_6I_9S (top) and $Nb_6(H)I_9S$ (bottom). Niobium atoms are open ellipsoids connected by heavy lines, the iodines have shaded octants, the sulfurs are solid, and the hydrogen atoms are striped. The intercluster Nb–Nb bonds (Nb2–Nb4 and Nb3–Nb6 in Nb_6I_9S; Nb2–Nb4 in $Nb_6(H)I_9S$) are outlined. Note that in the hydride there are weaker positive overlap populations also for the two remaining intercluster interactions (dotted lines).

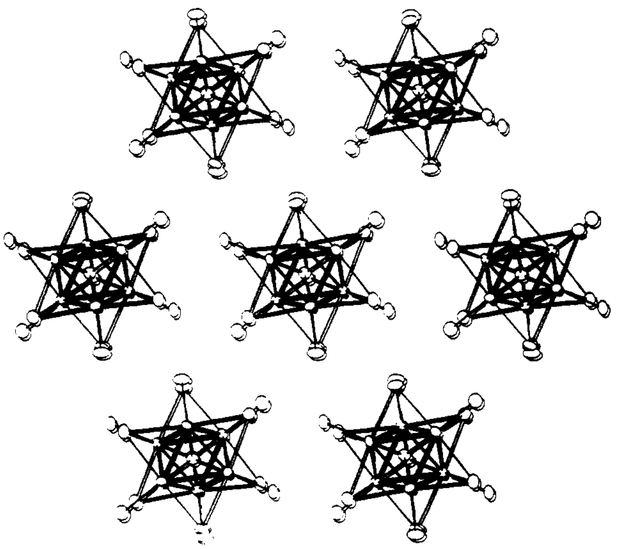

Figure 2. Approximate [111] view of the structure of Nb_6I_9S.

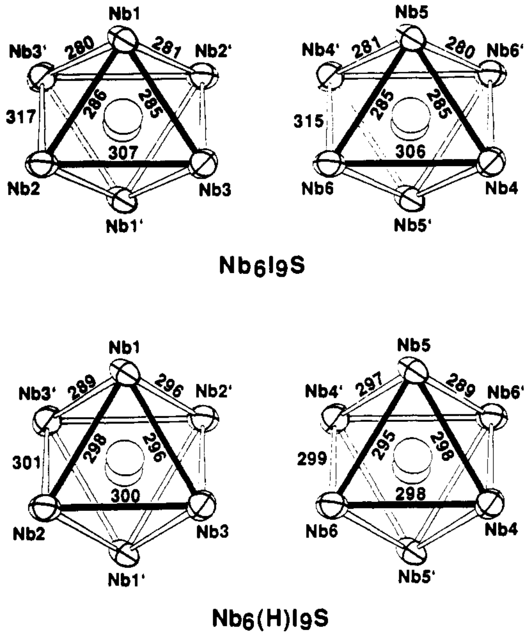

Figure 3. Two slightly distinct niobium octahedra ($Nb_6S_{2/2}$) in Nb_6I_9S and its hydride, with bond distances in pm. Each cluster contains a center of symmetry.

Table I. Important Intercluster Distances (pm)[4]

atom	distances		
	Nb_6I_9S	$Nb_6(H)I_9S$	ideal[a]
Nb1–Nb5	396.5 (2)	355.7 (4)	357
Nb2–Nb4	335.8 (2)	340.9 (4)	357
Nb3–Nb6	337.4 (2)	350.9 (4)	357
Nb1–S	253.6 (5)	246.7 (7)	245
Nb2–S	240.8 (5)	243.0 (7)	245
Nb3–S	241.0 (5)	244.9 (7)	245
Nb4–S	241.7 (5)	243.6 (7)	245
Nb5–S	254.4 (5)	246.4 (7)	245
Nb6–S	241.5 (4)	245.4 (7)	245

[a] Intracluster Nb–Nb distances were set to 292 pm.

iodine s and p orbitals. The contributions of these orbitals are shown in the density of states projection (DOS) in Figure 4. The ordering of states in the area shown is sulfur s, iodine s, sulfur p/iodine p and niobium d with increasing energy. In $Nb_6(H)I_9S$ we note an additional block at about −15.7 eV of a mixed Nb (d,s,p)–H (s) nature. The lower iodine and sulfur states contain some metal contributions forming the bonding metal–iodine and metal–sulfur combinations. The metal d-block is split at around −7.5 eV. The lower part is mainly metal–metal bonding (iodine and sulfur contributions are negligible here) and is formed by 24 energy bands (two clusters that could accommodate a maximum of 24 electrons each). Differences in the DOS are rather gradual for the idealized structure of Nb_6I_9S and the real structures of $Nb_6(H)I_9S$ and Nb_6I_9S. Our point of interest is the lower d-block, with the band structures shown in Figure 5.

Metal–metal interactions within the pairs of clusters are build up mainly from 12 × 5 d orbitals in bonding and antibonding combinations. Considering a threefold symmetry along the chain axis, 20 **a** states and 20 **e** states are obtained from orbital mixing. Eight of each belong to the metal–metal bonding block, with a maximum capacity for 48 electrons (24 per cluster). The ordering of energy levels of the lower d states for a molecular $(Nb_6I_6S_2)I_6^{5-}$ fragment is shown in Figure 6. There are changes mainly of some **a** energy levels, due to intercluster metal–metal interactions on going to the extended structure. In particular, one of the a_{1g} states is raised in energy once its d_{z^2} orbitals interact with neighboring clusters along the infinite chain. Of course, the 2-fold degeneracies remain preserved in the band structure of the idealized infinite chain. The bands have a folded appearance as a result of the 6_3 screw axis relating two identical clusters within the repeat unit. Thus, each band has a counterpart of qualitatively the same contribution of orbitals along the **k** vector, and the zone edge contains 2-fold and 4-fold degeneracies. These degeneracies are sensitive to the symmetry reduction found in the structures of $Nb_6(H)I_9S$ and Nb_6I_9S, and supposedly to electron counts below 24 per cluster.

The section of interest of the band structures is located near the fermi level. In Nb_6I_9S 2 × 19 electrons and in $Nb_6(H)I_9S$ 2 × 20 electrons occupy the d bands (Figure 5). Note that in the band structure of $Nb_6(H)I_9S$ two of these bands have disappeared owing to the interaction with hydrogen, as discussed later.

Neither 3-fold nor 6_3 symmetry is retained in the structures of $Nb_6(H)I_9S$ and Nb_6I_9S and, consequently, no degeneracies (along **k** or at the zone edge) and no crossings of bands are allowed. But still the band structures exhibit signatures of the idealized model.

The section of the band structure around the Fermi level of the idealized structure, emphasized in Figure 7, contains two 2-fold degenerate bands running into a 4-fold degeneracy at the A point. Considering 20 electrons per cluster, the lower degeneracy is filled (bands 99 and 100) and the upper (folded) bands (101 and

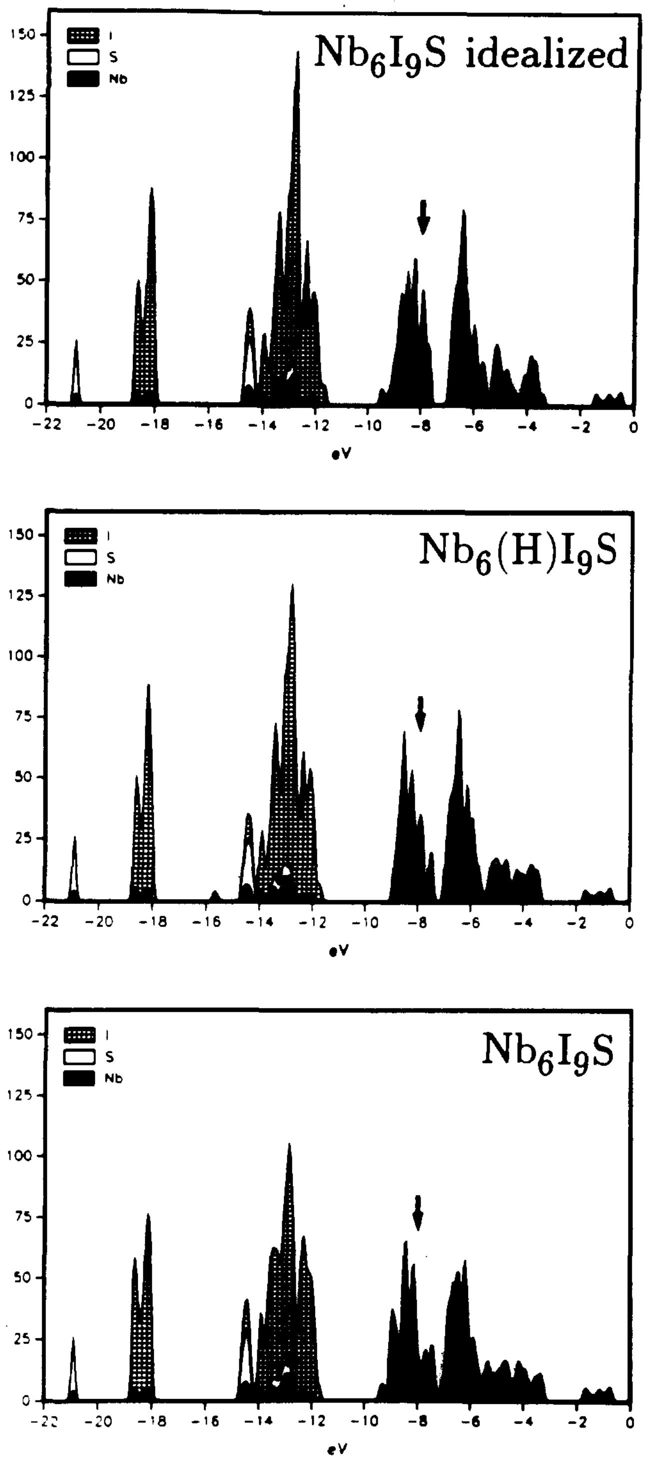

Figure 4. Density of states (DOS) projection of Nb_6I_9S (idealized), $Nb_6(H)I_9S$ and Nb_6I_9S. The Fermi levels are marked by arrows.

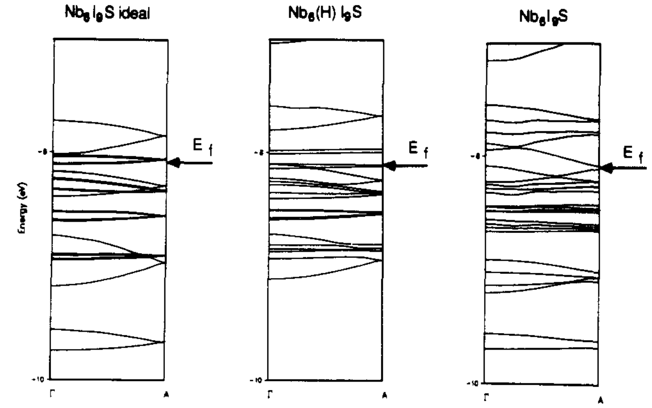

Figure 5. Band structure diagrams of the bonding d-block in Nb_6I_9S (idealized), $Nb_6(H)I_9S$ and Nb_6I_9S. The Fermi levels are marked by arrows. Two d-bands of the hydride are lowered by interaction with the hydrogen (see text).

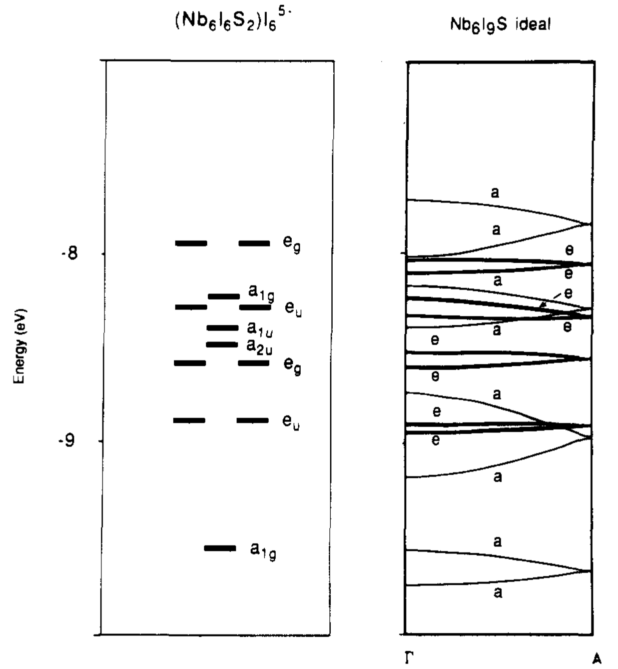

Figure 6. Molecular orbital diagram for an idealized $(Nb_6I_6S_2)I_6^{5-}$ fragment in comparison with a section of the band structure of the idealized Nb_6I_9S cluster.

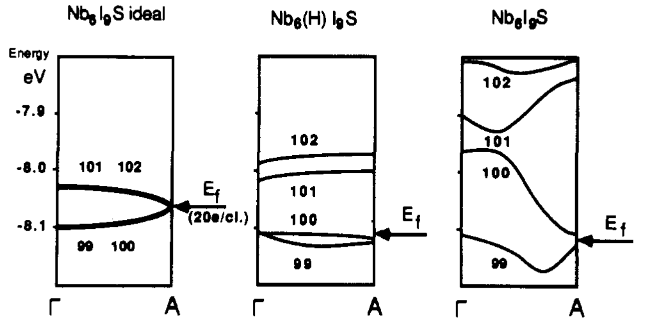

Figure 7. Section of the band structures (and their numbers) at the Fermi level. The Fermi level for 20-, 20-, and 19-electron clusters are marked by arrows.

102) are empty. For this occupancy, with the same electron count as in $Nb_6(H)I_9S$, a typical Peierls[10] distortion is expected and is indeed what we find. The distortion of the chain splits the former 4-fold degeneracy at the A point, stabilizing the occupied bands and raising the empty bands in energy (Figure 7, middle). The splitting of bands is clearly introduced by the arrangement of Nb atoms, because iodine and sulfur orbitals barely have a contribution to these states. The distortion present in the $Nb_6(H)I_9S$ structure causes a loss of the 3-fold symmetry in each single cluster and thus a splitting of degeneracies along the **k** vector. More importantly, this type of stabilization gains from the deviation from the (6_3) screw relationship between clusters, breaking the degeneracies at the A point.

Going to the more distorted Nb_6I_9S, we find a coincident trend at the Γ and A points, already noted in the hydride, but with different consequences. At the A point, bands split successively with the deviation from the 6_3 relationship between the clusters, lowering bands 99 and 100 and increasing bands 101 and 102 in

---

[10] Peierls, R. E. Quantum Theory of Solids, Oxford University Press, Oxford, U.K., 1972.

energy. At the Γ point, the formerly degenerate bands split off successively with the distortion of the clusters, increasing bands 100, 101, and 102 and lowering band 99 in energy. Relative to 20 electrons, as present in the hydride, this band arrangement is less favored, but for 19 electrons per cluster (in Nb_6I_9S), stabilization is obtained by lowering the highest occupied band (99) and raising the lowest unoccupied band (100) in energy. Therefore, the smaller cluster distortion in the hydride is demanded electronically and not necessarily from a steric claim of the interstitial hydrogen atom.

Overlap Populations

A calculation of the crystal orbital overlap populations (COOP) for the Nb–Nb and Nb–S (Nb–H) bonds was used to evaluate the bonding characteristics of Nb_6I_9S and $Nb_6(H)I_9S$ in comparison with that in an idealized model. The distance parameters used for the idealized structure were adapted from averaging the distances in Nb_6I_9S (Table I).

In the idealized structure, we note two basic trends on filling electrons successively from 19 electrons per cluster (band 99) up to 24 electrons per cluster. The Nb–S and the intercluster Nb–Nb overlap populations decrease slightly from 0.36 to 0.34 and from 0.04 to 0.01, respectively, and the intracluster Nb–Nb populations increase.

In the distorted structures, the overlap populations differ for every bond. However, the average overlap population per bond remains the same, i.e. 0.21 for $Nb–Nb_{intra}$ and 0.36 for Nb–S in the 19 electrons per cluster idealized structure and in Nb_6I_9S. But we note a drastic increase in overlap populations for the two short intercluster Nb–Nb bonds in the distorted Nb_6I_9S, which become almost 50% of an average Nb–Nb intracluster bond. The $Nb–Nb_{inter}$ overlap populations are 0.10 each (and 0.0 for one longer Nb–Nb contact), decreasing to 0.05 (–0.03) for 24 electrons per cluster.

Because of the expansion of the clusters in $Nb_6(H)I_9S$ (20 electrons per cluster), the average Nb–Nb overlap population per bond is only 0.20, while it is 0.24 in the ideal cluster with the same number of electrons. But strong Nb–H overlap populations are present in the hydride, averaging to 0.11 per Nb–H. The average overlap populations (20 electrons per cluster) per bond for Nb–S and intercluster Nb–Nb contacts are identical with values noted above for 19 electrons per cluster. Consistent with the Nb–Nb bond distances in the hydride (Table I), we note one stronger (0.09) and two weaker (0.05, 0.06) intercluster Nb–Nb interactions.

Influence of Hydrogen

Two low-lying a_{1g}-like bands located in the d-block of two Nb_6I_9S clusters strongly interact with two hydrogen s orbitals, to give two bonding and two antibonding states in $Nb_6(H)I_9S$. These states are well separated from the d-block and exhibit metal–metal and metal–hydrogen characteristics. The bonding interaction is located below the p-block of I and S at about –15.7 eV. Only the metal contributions to these states are shown in Figure 4. The unoccupied antibonding combinations are raised above the Fermi level. Thus, the number of bands up to the Fermi level remains unchanged and only the number of electrons is increased from 19 to 20 electrons (per cluster) by the electron provided by the hydrogen atom. A similar feature has been noted with $Nb_6(H)I_{11}$.[11] However, $Nb_6(H)I_9S$ as well as $Nb_6(H)I_{11}$ may be viewed as 18-electron cluster compounds if we neglect the metal contributions to the a_{1g}-like bands. This view would consider these bands as pure hydrogen states and would take into account only electrons occupying d-bands located above the halide p-bands in energy.

This type of interaction is also obtained in other hydrogen centered clusters of octahedral symmetry i.e., in $Zr_6(H)Cl_{12}$,[12] where the low-lying metal-based a_{1g} state is lowered by the bonding interaction with the hydrogen s orbital.

Distortion and Conductivity

The hypothetical, undistorted structure may be regarded as an insulator with 24 electrons in metal–metal bonding states per cluster, as obtained for $Mo_6I_8Se_2$.[8] The latter was reported to have the same basic structure as the niobium compound, with one selenium atom statistically occupying iodine positions. Some structural details, however, remain uncertain in terms of symmetry and distortion.

For 20 electrons per cluster in the undistorted structure, bands 99 and 100 are filled, yielding a local half-filled block. Splitting of the 4-fold degeneracy (distortion) at the A point yields a stabilization of the two filled bands, increasing the empty bands (101 and 102) in energy. Thus, in $Nb_6(H)I_9S$ a band gap of the order of <0.1 eV opens up. Upon further distortion, the splitting at the A point increases, successively lowering bands 99 and 100. For 19 electrons per cluster the highest occupied band (99) at Γ lies at about at the same energy as the lowest unoccupied band (100) at the A point, Figure 7. This band overlap would represent a semimetal. In case we consider this indirect band gap not to be significant, the compound would be a semiconductor with a calculated band gap of the order of 0.03 eV. However, our calculations cannot be trusted to yield relative energies accurate enough to decide between these. In any case, we do not believe that one conduction mechanism will be present here without the other. The conductivity measurement revealed a semiconductor-like temperature dependency, accompanied by an almost metal-like magnitude in conductivity of the order of 30 Ω^{-1} cm^{-1} at room temperature.[4] Both compounds show a temperature-independent Pauli-like paramagnetism in the temperature range of ~20–400 K.[13]

Conclusions

According to our calculations, the distortions in the one-dimensional chain compounds Nb_6I_9S (19 electrons) and $Nb_6(H)I_9S$ (20 electrons) are driven electronically by a local half-filled block, splitting successively with increasing distortion. The distortion in the hydride is relatively small, yielding a band splitting at the zone edge on the order of 0.1 eV, increasing to almost 0.4 eV in the strongly distorted Nb_6I_9S.

$Tl_2Mo_6Se_6$[14] and $LiScI_3$[2,15] do not undergo a distortion even though the band structures favor Peierls distortions. Metal atoms located in the channels of these structures might be responsible for an interchain coupling, not possible in the title compounds.

Bonding along the chains in the title compounds arises from Nb–Nb interactions within the clusters that dominate the band structure around the Fermi level. Very weak metal–nonmetal interactions in this area are mainly antibonding, giving a slight dispersion to the metal-based bands in this region, while strongly bonding Nb–I and Nb–S interactions fall at lower energies. Intercluster Nb–Nb bonding appears to be negligible in the idealized structure but becomes notable in the distorted compounds. In Nb_6I_9S, two intercluster Nb–Nb bonds are present with correspondingly short contacts. However these bonds are only about half as strong as a typical Nb–Nb bond.

The idealized structure seems to be favored by 24 electrons per cluster, as would be obtained with nitrogen atom in the interstitial cluster center. Up to this level all metal-based bands are mainly bonding, well separated from the antibonding bands by a gap on

---

[11] Simon, A. *Ann. Chim. Fr.* **1982**, *7*, 539.

[12] Hughbanks, T. *Prog. Solid State Chem.* **1989**, *19*, 329.

[13] Miller, L. L. Private communication.

[14] Hughbanks, T.; Hoffmann, R. *Inorg. Chem.* **1982**, *21*, 3579.

[15] Lachgar, A.; Dudis, D. S.; Dorhout, P. K.; Corbett, J. D. *Inorg. Chem.* **1991**, *30*, 3321.

Table II. Extended Hückel Parameters

atom	orbital	H_{ii}, eV	$\zeta_1{}^a$	ζ_2	$c_1{}^b$	c_2
Nb	4d	−8.26	4.08	1.64	0.6401	0.5510
	5s	−7.92	1.89			
	5p	−4.15	1.85			
S	3s	−20.00	2.12			
	3p	−13.30	1.83			
I	5s	−18.00	2.68			
	5p	−12.70	2.32			
H	1s	−15.00	2.20			

[a] Slater type orbital exponent. [b] Coefficients used in double ζ expansion.

the order of 0.8 eV, depending on the distance parameters in the structure. In the actual $Nb_6(H)I_9S$ and Nb_6I_9S some d states become partially antibonding and therefore broaden above −8 eV.

Along the infinite chain direction, the calculated band structure reveals Nb_6I_9S to be a semiconductor or close to a semimetal, while $Nb_6(H)I_9S$ is a semiconductor, whereas both compounds in directions orthogonal to the infinite chains should behave as insulators.

Acknowledgment. We are indebted to A. Guloy for valuable advice on several points and to L. Miller for the magnetic studies on Nb_6I_9S and $Nb_6(H)I_9S$. This research was supported by the Deutsche Forschungsgemeinschaft and by the National Science Foundation, Solid State Chemistry, via Grant DMR-8902954, and was carried out in part in the facilities of the Ames Laboratory, DOE.

Appendix

The extended Hückel method[9] was used for the one-dimensional calculations using a set of six **k** points.

Calculations of the band structure of Nb_6I_9S were done using 188 orbitals, and the orbital parameters given in Table II. The Nb 5p orbitals were not used in early calculations and are not contained in the DOS shown. Inclusion of Nb 5p orbitals introduced only small changes in the bands and in the overlap populations.